






eXplainable Artificial Intelligence Framework for Structure's Limit Load Extimaton

Habib Imani³^a, Renato Zona¹^b, Armando Arcieri⁴, Luigi Piero Di Bonito²^c,
Simone Palladino¹^d and Vincenzo Minutolo¹^e

¹Department of Engineering, Università della Campania Vanvitelli, Via Roma 29, Aversa (CE), Italy

²Dipartimento di Ingegneria Chimica, dei Materiali e della Produzione Industriale, Università degli Studi di Napoli "Federico II", Naples, Italy

³Department of Engineering and Architecture, Università degli Studi di Catania, Via S. Sofia 64, Catania (CT), Italy

⁴Independent Researcher, Italy


Keywords: Machine Learning, Finite Element, Limit Analysis, Virtual Twin, Vulnerability.


Abstract: The recent advancements in machine learning (ML) and deep learning (DL) have significantly expanded opportunities across various fields. While ML is a powerful tool applicable to numerous disciplines, its direct implementation in civil engineering poses challenges. ML models often fail to perform reliably in real-world scenarios due to lack of transparency and explainability during the decision-making process of the algorithm. To address this, physics-based ML models integrate data obtained through a finite element procedure based on the lower bound theorem of limit analysis, ensuring compliance with physical laws described by general non-linear equations. These models are designed to handle supervised learning tasks while mitigating the effects of data shift. Widely recognized for their applications in disciplines such as fluid dynamics, quantum mechanics, computational resources, and data storage, physics-based ML is increasingly being explored in civil engineering. In this work, a novel methodology that combines machine learning and computational mechanics to evaluate the seismic vulnerability of existing buildings is proposed. Interesting and affordable results are reported in the paper concerning the predictability of limit load of structure through ML approaches. The aim is to provide a practical tool for professionals, enabling efficient maintenance of the built environment and facilitating the organization of interventions in response to natural disasters such as earthquakes.


1 INTRODUCTION


Machine Learning (ML) and Deep Learning (DL), such as deep neural networks (DNNs), are increasingly integrated into the scientific process, replacing traditional statistical methods and mechanistic models across various sectors and fields, including education (Momeny et al., 2021), natural and environmental sciences (Malami et al., 2021; Campanile et al., 2024), medicine (Sharma et al., 2021; Vadyala and Sherer, 2021), engineering (Santhosh et al., 2021; Campanile et al., 2023; Di Bonito et al., 2023), and social sciences (Ciaccio and Troisi, 2021). In civil engineer-


ing, where mechanistic models have historically prevailed, ML is also gaining traction (Vadyala et al., 2021, 2022). Despite its growing adoption, ML methods are often criticized by researchers and end users as a "black box," as they provide inputs and outputs without offering physically interpretable insights to the user (McGovern et al., 2019). This critique has driven some scientists to eXplainable Artificial Intelligence (XAI) models to address concerns regarding the opacity of black-box methods (Gunning and Aha, 2019; Alber et al., 2019; Laub, 1999; Karpatne et al., 2017). In civil engineering, ML models are generated directly from data through algorithms, yet even their developers often struggle to fully understand how input variables are combined to produce predictions. While these models identify relevant input variables, their complexity makes it difficult to discern the interactions that lead to final predictions. In this con-

^a <https://orcid.org/0009-0004-6455-3779>

^b <https://orcid.org/0000-0001-6718-9387>

^c <https://orcid.org/0000-0001-5002-4789>

^d <https://orcid.org/0000-0001-6718-9387>

^e <https://orcid.org/0000-0002-7787-4844>

text, the development of XAI plays a crucial role in improving the trustworthiness and robustness of both ML and DL models, particularly for critical applications where safety is a key concern (Di Bonito et al., 2024). For instance, ML models that fail to accurately estimate structural damage are often associated with processes that are not entirely understood and present challenges such as high data requirements, difficulty in providing physically consistent findings, and limited generalizability to out-of-sample scenarios. Large, curated datasets with well-defined, precisely labeled categories are typically used to evaluate ML and DL models (Momeny et al., 2021). While DL performs well under such conditions, it assumes a relatively stable environment. The environment boundary conditions are taken into account. Soil structure interaction is a future perspective to be considered. Recent developments in soil identification (Damiano et al., 2024; de Cristofaro et al., 2024) suggest to consider the soil as a detailed boundary condition. In this paper a well-established procedure (Zona and Minutolo, 2024) was used to construct a reference database for the limit load assessment of frame structures. The aim was to obtain an initial approach to the calculation based on post-hoc XAI methodology (Barredo Arrieta et al., 2020) to assess the reliability of the results when varying various predefined parametric conditions.

2 FROM FINITE ELEMENT LIMIT ANALYSIS TO MACHINE LEARNING

This paper introduces a methodology to determine the limit load of civil structures under standard loading conditions. The objective is to develop a tool that surpasses conventional approaches to assess the ultimate strength of structures. A detailed description of an alternative computational procedure, different from those outlined in current standards, is provided in Mangalathu et al. (2020). The advancement of this methodology lies in the use of the limit load as a parameterized indicator of seismic vulnerability. The shift from traditional computational mechanics to Computational Mechanics 3.0 is facilitated through the application of machine learning algorithms. These algorithms enable the generation of reliable and actionable results for managing seismic emergency scenarios in a significantly shorter timeframe compared to classical computational methods. The seismic risk classification for individual buildings—critical for predicting potential earthquake impacts—relies on

structural resistance characteristics derived from geometry and material properties. This process establishes qualitative assessment criteria through site inspections and surveys, factoring in building typology, construction date, and the regulations in effect during the building's erection. These criteria help extract quantitative data on mechanical properties, which can then be applied to simplified analytical models.

The conducted surveys aim to develop representative numerical models that enable rapid and reliable assessments of structural resistance and vulnerability. At the building scale, structural characterization is achieved by analyzing and categorizing settlements into homogeneous groups based on the following parameters:

- Geometric configuration
- Construction date (age of the structure and building methods)
- Regulatory framework at the time of construction, providing insights at the broader building sector level
- Neighborhood context and its influence on expected vulnerability

This data supports the creation of a numerical twin for each building type (morphotype), allowing the identification of zones with comparable risk parameters. Consequently, seismic micro-zoning can be implemented, focusing on structural vulnerabilities. By applying micro-zoning at a micro-seismic scale, it becomes possible to assess earthquake effects through qualitative and topological classifications of building vulnerabilities, considering both existing damage and potential future risks. Ultimately, the goal is to develop simplified strategies for evaluating and analyzing structural performance. These strategies rely on indirect assessments, enabling the interpretation of a building's structural behavior through quantitative parameters derived from observations and simplified measurements across building clusters.

2.1 Finite Element Limit Analysis via VFEM Methodology

This analytical approach employs a static limit analysis framework implemented through specialized finite element procedures. The method establishes the mathematical foundation for self-equilibrated stress fields (Zona et al., 2021) through linear optimization techniques (VFEM protocol) (Zona and Minutolo, 2024). The formulation originates from Volterra dislocation theory, utilizing isoparametric shape functions that map discontinuous displacement fields through nodal parameters.

The computational core implements an optimization routine that determines the critical load multiplier by evaluating statically admissible solutions, with Melan residuals expressed as nodal dislocation parameters. The stress-strain relationship derives from strain representations generated through shape function derivatives, accommodating various structural models through adaptable element formulations. Displacement-based nodal parameters simultaneously characterize internal dislocation patterns, creating a unified FEM framework that links self-equilibrated stresses to nodal variables. This formulation enables direct limit load calculation through constrained optimization:

$$s_\alpha = \sup_{\delta} k, \quad | \quad (k\sigma^* + \mathcal{V}\delta) \in D_e, \quad (1)$$

$$\alpha = \begin{cases} sd, & \text{shakedown} \\ c, & \text{collapse} \end{cases}$$

where the eigenstress field emerges from the nodal mapping (1):

$$\sigma^0 = \mathcal{V}\delta \quad (2)$$

The singular matrix \mathcal{V} relates element stress vectors to nodal parameters δ . This methodology eliminates conventional limitations requiring detailed load history knowledge, particularly advantageous for structures subjected to stochastic loading scenarios. Melan's approach proves robust against load path uncertainties, focusing instead on critical load patterns and intensity domains. The framework enables comprehensive safety assessment through parametric studies across structural morphotypes. Key vulnerability indicators include:

- Span configurations in principal directions
- Vertical height-to-span ratios
- Relative strength of vertical vs. horizontal members

Through a comprehensive computational approach, the structural safety level can be estimated based on both load and displacement parameters. This methodology involves a parametric analysis of numerous numerical experiments conducted on various structural types, leading to the development of risk abacuses. The procedure encompasses modeling structures with diverse morphological and topological characteristics while thoroughly examining their structural responses. For each structural morpho-type, the capacity curve is defined based on its key parameters. The safety factor for each morpho-type is then precisely determined based on influential parameters such as the number of spans in the primary structural layout directions, the overall height, and the strength ratios

of columns and beams. The key parameters characterizing the capacity curve—safety factor, ultimate displacement at collapse, and residual displacements related to residual stresses—allow for direct comparisons among different morpho-types. This comparative analysis facilitates the assessment of structural vulnerability across various building groups.

2.2 Finite Element Limit Analysis (FELA) Formulation

A stress field, σ_a , is considered statically admissible if it satisfies the equilibrium conditions while remaining confined within the domain D_e .

$$\sigma_a = (\sigma^* + \sigma_0) \in (\mathcal{E}_t \cap \mathring{D}_e) \quad (3)$$

The Greenberg-Prager lower bound theorem in limit analysis states that a load in equilibrium with a statically admissible stress does not result in structural collapse. Furthermore, if the material adheres to the Drucker stability condition and the load can be expressed using a multiplicative factor k such that $\sigma(t) = k\sigma^*(t) + \sigma_0(t)$, then the ultimate load corresponds to the supremum of k .

Several important phenomena are encompassed in this description. Specifically, when a unique load pattern is applied and the multiplier k serves as a monotonically increasing parameter, the supremum of k defines the collapse threshold. Beyond this straightforward case, when a structure experiences multiple load patterns whose intensities can be bounded by a common scalar factor k , additional failure mechanisms such as shakedown, ratcheting, and low-cycle fatigue must also be considered, provided that the stress envelope throughout the structure's time history is properly accounted for.

In all scenarios, determining the load limit reduces to solving an optimization problem in terms of the time-independent eigenstress $\bar{\sigma}_0$, as summarized in the following equation:

$$s_\alpha = \{ \sup_{\Sigma_0} k | (k\sigma^* + \bar{\sigma}_0) \in D_e \}, \quad (4)$$

$$\alpha = \begin{cases} sd & \text{shakedown} \\ c & \text{collapse} \end{cases}$$

Defining a discretized form of the eigenstress domain, where the solution is to be sought, is essential for determining the load limit using the finite element method (FEM).

The formulation adopted in this study, as presented in Zona and Minutolo (2024), expresses eigenstress in terms of a set of nodal parameters δ , which represent eigenstrain as a dislocation distribution within the elements.

$$\sigma^0 = \mathcal{V}\delta \quad (5)$$

Based on equation (5), if there exists a nodal parameter set $\hat{\delta}$ that ensures the stress remains within the elastic domain at every stage of the load path, the structure avoids an unbounded accumulation of plastic strain. Consequently, failure due to collapse, alternating plasticity, or ratcheting does not occur.

The load limit multiplier is obtained as the supremum of the load multipliers in the constrained optimization problem (4), modified according to equation (5), as follows:

$$s_{\alpha} = \sup_{\delta} k | (k\sigma^* + \mathcal{V}\delta) \in D_e, \quad (6)$$

$$\alpha = \begin{cases} sd & \text{shakedown} \\ c & \text{collapse} \end{cases}$$

The matrix \mathcal{V} is singular, with two dimensions corresponding to the size of the element stress vector and δ , respectively. The rank of \mathcal{V} represents the number of independent solutions to the equilibrium equations and aligns with the structural redundancies. In trusses and frames, this rank is finite and independent of discretization, whereas for other structural systems, it is inherently infinite. When discretization is applied, the rank becomes finite and depends on the chosen discretization scheme. However, in general, the rank of \mathcal{V} remains lower than its total dimensions.

Different constitutive models define distinct domains, which impose constraints on the optimization procedure. The constraint inequalities utilized in the calculations have been linearized by approximating the domain with an inscribed polyhedron. In the case of plane stress conditions, this linearized domain forms an octahedron that matches the nonlinear domain at its intersections with the coordinate axes, leading to the following set of linear inequalities:

$$\sum_i \prod_{j \in \{i\}} \sigma_{j\beta_r} \sigma_i \leq \prod_j^n \sigma_{j\beta_r} \quad (7)$$

The expression in (7) consists of f inequality constraints, where $r = \{1, \dots, f\}$, positioned at the faces of the polyhedron. For an octahedral domain under plane stress conditions, $f = 8$. These constraints (7) are applied at the nodal points of the finite element model. Given that the actual stress σ_i has been decomposed according to equation (5), the optimization problem is reformulated as a linear programming problem:

$$\sup_{\delta} k \left| \sum_i \prod_{j \in \{i\}} \sigma_{j\beta_r} (k\sigma^* - \mathcal{V}\delta)_i \leq \prod_j^n \sigma_{j\beta_r} \quad (8)$$

When the applied loads are divided into a constant dead load and a live load that can increase with a multiplier k , the stress is split into a fixed part σ^p and a

variable part $k\sigma^h$. The stress representation is then modified as:

$$\sigma = \sigma^p + k\sigma^h + \mathcal{V}\delta$$

Consequently, the compatibility inequalities are transformed to:

$$\sup_{\delta} k \left| \sum_i \prod_{j \in \{i\}} \sigma_{j\beta_r} (k\sigma^h + \mathcal{V}\delta + \sigma^p)_i \leq \alpha \prod_{j=1}^n \sigma_{j\beta_r} \right.$$

The solutions obtained from the optimization programs in (8) provide the load multiplier at the collapse or shakedown limit.

In the present analysis, the finite element discretization is composed of two-dimensional isoparametric 4-node linear elements. The input routines were generated using the Ansys© preprocessor macro, which produced database files containing node coordinates, element connectivity, material properties, and applied loads. This data was subsequently processed within a custom procedure for limit analysis. The developed routine assembled the required matrices, computed the elastic stress state, formulated the constraints for the optimization problem, and determined the ultimate load multiplier through an optimization-based approach.

The geometric interpretation of the compatibility constraints is illustrated in Figure 1. It can be observed that employing a linearized domain results in a conservative estimate of the structural strength. To mitigate this underestimation, a correction factor is introduced. As discussed in (Zona and Minutolo, 2024) and demonstrated in Figure 2, an amplification factor is applied along the actual stress trajectory. This factor corresponds to the ratio between the distance from the origin to the plane parallel to the polyhedral face, where the extended stress vector intersects the nonlinear domain, and the corresponding linearized polyhedral face, as depicted in Figures 1 and 2.

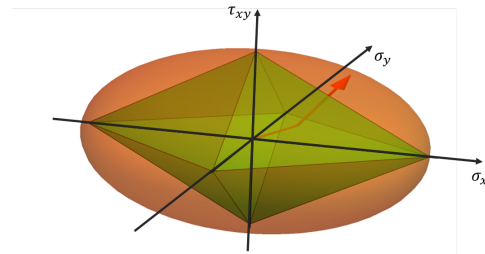


Figure 1: Linearized limit domain inscribed in the ellipsoid.

$$\alpha = \frac{d_{\alpha}}{d} > 1 \quad (9)$$

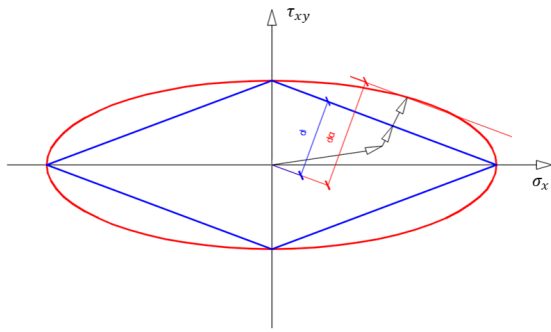


Figure 2: Geometric representation of the α factor.

2.3 Database Construction

For performing linear static analysis on the frames, the VFEM routine was utilized. The procedure follows a structured approach: initially, the frame model is developed using FEM software, which serves exclusively as a CAD interpreter. This method simplifies the specification of nodal connectivity, element types, and boundary conditions. Additionally, an automated routine was implemented to generate various frame configurations, which are subsequently analyzed and compiled into a results table that forms the basis of the vulnerability assessment.

The FELA routine computes the load multiplier at the elastic limit, the collapse load multiplier, and the maximum elastic displacements. These results are systematically stored in a tensor, encapsulating data for each morphological frame type. The overall workflow is illustrated in Figure 5.

A CAD compiler enables an automated procedure for evaluating various structural configurations. Specifically, a series of structures is generated with different numbers of floors, columns, and column spacing. The output filename of each frame encodes its corresponding geometric characteristics:

$$\text{VirtualTWIN}_{i-j-h-k-l-m} \quad (10)$$

- $i \rightarrow$ number of pillars in the x direction
- $j \rightarrow$ number of pillars in the z direction
- $h \rightarrow$ number of floors in the y direction
- $k = 3 \rightarrow$ distance between each floor
- $l \rightarrow$ distance between pillars in x direction
- $m \rightarrow$ distance between pillars in z direction

An essential parameter in virtual twin modeling is the cross-sectional dimensions of beams and columns. In this study, a cross-section of 60×40 cm is adopted.

The collapse multiplier results are obtained by considering the specialized limit domain. To compute the collapse multiplier, an optimization routine

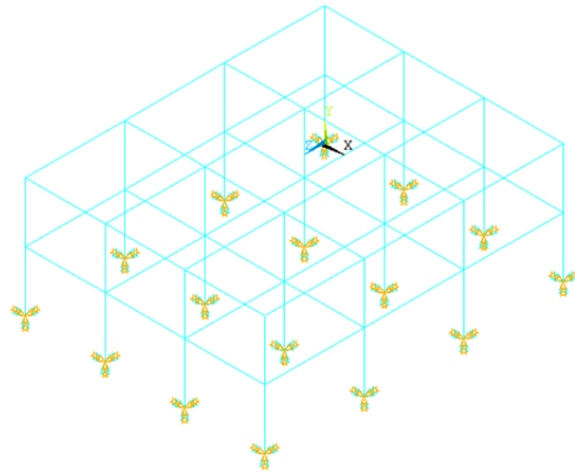


Figure 3: VirtualTWIN: $i=4, j=4, h=2, k=3, l=m=4$.

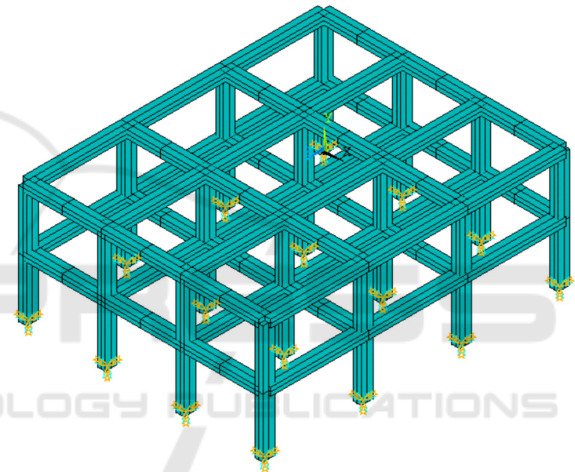


Figure 4: VirtualTWIN with (60x40) cm cross-section.

based on linear programming is employed, solving a constrained optimization problem with a linear objective function and linear constraints. In the present case, the constraints are defined by the boundary of the limit domain, while the objective function corresponds to the collapse multiplier.

For the application of linear programming, the plastic compatibility domain of a generic beam section under biaxial bending, characterized by three stress components, is linearized using a flat-plane approximation. Specifically, eight planes, each corresponding to one of the faces of a non-regular octahedron tangential to the curved domain, are utilized. Although the domain can be enveloped with multiple flat layers without compromising the algorithm's fundamental properties, this approach introduces additional computational complexity.

Consequently, the boundary polyhedron faces are characterized by six distinct boundary stress values: $M_{yu}, M_{ycu}, M_{zu}, M_{zcu}, N_{tu}, N_{cu}$. The subscripts of

**Evaluation of Vulnerability
brief scheme**

Morpho-type definition

- Geometry (base, height, horizontal symmetry, vertical symmetry)
- Construction age (legislation in force at the time of construction)
- Material (different concrete type)

DataBase Construction

- VirtualTWIN random generation
- VFEM approach to define ductility requirement : Simplified Pushover Analysis
- Results Collection and Normalization

SafeScore

- SafeScore definition through weighted parameters
- Risk Vulnerability Class Attribution

Figure 5: Procedure Workflow.

these stresses denote the direction of the acting moments (y or z) and whether the stress corresponds to tension or compression (t/c) based on the positive or negative intersection with the respective axis. This formulation allows the planes of the octahedron to be represented through the following equations:

$$\frac{M_y}{M_{y\beta u}} + \frac{M_z}{M_{z\beta u}} + \frac{N}{N_{\beta u}} = 1 \tag{11}$$

where $\beta = t$ or c , and the quantities in the denominator take the values specified above, while the terms in the numerator represent the stresses obtained from the structural analysis.

The generic stress can be formulated as a combination of the corresponding components of V and the amplified elastic rate associated with an arbitrary multiplier k .

$$M_y = V_{M_y} \delta + kM_y, \quad M_z = V_{M_z} \delta + kM_z, \quad N = V_N \delta + kN \tag{12}$$

The previously mentioned positions, when substituted into the equation 11, offer a representation based on stress parameters. Being part of the internal limit domain of the loading is equivalent to fulfilling the inequalities of the linearized domain, which are expressed by the following eight matrix inequalities in terms of δ and k .

The optimization problem associated with the static theorem (in Melan’s form) involves finding the maximum value of k subject to the following con-

straints:

$$\begin{aligned} & \left(\frac{V_{M_y} \delta + kM_y}{M_{ytu}} + \frac{V_{M_z} \delta + kM_z}{M_{ztu}} + \frac{V_N \delta + kN}{N_{tu}} \right) < 1 \\ & \left(\frac{V_{M_y} \delta + kM_y}{M_{ycu}} + \frac{V_{M_z} \delta + kM_z}{M_{ztu}} + \frac{V_N \delta + kN}{N_{tu}} \right) < 1 \\ & \left(\frac{V_{M_y} \delta + kM_y}{M_{ytu}} + \frac{V_{M_z} \delta + kM_z}{M_{zcu}} + \frac{V_N \delta + kN}{N_{tu}} \right) < 1 \\ & \left(\frac{V_{M_y} \delta + kM_y}{M_{ycu}} + \frac{V_{M_z} \delta + kM_z}{M_{ztu}} + \frac{V_N \delta + kN}{N_{cu}} \right) < 1 \\ & \left(\frac{V_{M_y} \delta + kM_y}{M_{ytu}} + \frac{V_{M_z} \delta + kM_z}{M_{zcu}} + \frac{V_N \delta + kN}{N_{cu}} \right) < 1 \\ & \left(\frac{V_{M_y} \delta + kM_y}{M_{ycu}} + \frac{V_{M_z} \delta + kM_z}{M_{ztu}} + \frac{V_N \delta + kN}{N_{cu}} \right) < 1 \\ & \left(\frac{V_{M_y} \delta + kM_y}{M_{ycu}} + \frac{V_{M_z} \delta + kM_z}{M_{zcu}} + \frac{V_N \delta + kN}{N_{cu}} \right) < 1 \\ & \left(\frac{V_{M_y} \delta + kM_y}{M_{ycu}} + \frac{V_{M_z} \delta + kM_z}{M_{zcu}} + \frac{V_N \delta + kN}{N_{cu}} \right) < 1 \end{aligned} \tag{13}$$

The procedure was implemented on a dataset consisting of 405 distinct structural morpho-types. The outcomes are presented in terms of SafeScore (SS), calculated as shown in Eq. (14):

$$SS = \alpha \cdot \beta \cdot \gamma \cdot \delta \cdot \eta \cdot \zeta \cdot S_{cVFEM} \tag{14}$$

The parameter S_{cVFEM} represent the collapse multiplier for each load case. In the case, the results are reported for the Permanent Load (self weight + additional load) and Seismic X and Seismic Z load. The

coefficients of the S_{CVFEM} represents respectively:

- $\alpha = \text{base regularity}$
- $\beta = \text{height regularity}$
- $\gamma = \text{base - height ratio}$
- $\delta = \text{age of construction}$
- $\eta = \text{cross - section}$
- $\zeta = \text{material}$

The initial set of results is presented in terms of elastic limit load, SE_i , collapse limit load, SC_i , and the ratio between SE and SC , denoted as R_i , where the subscript $i = \{1, 2, 3\}$ is defined as:

$$\begin{cases} i = 1 & \text{gravity load} \\ i = 2 & \text{seismic load in x direction} \\ i = 3 & \text{seismic load in z direction} \end{cases}$$

The objective is to enhance the calculation methodology by integrating the most advanced techniques in Machine Learning and deep learning, using the structured database described. The database incorporates input data for 405 frames:

- number of pillars in the two plane directions
- number of floors
- ultimate bending moments
- ultimate normal stress resistance
- section of the beams
- Area
- Inertia

The anticipated output is the limit resistance of the structures under various loading conditions, specifically vertical load simulating self weight of the structure and seismic load.

3 eXplainable ARTIFICIAL INTELLIGENCE

3.1 Dataset Description

The initial phase involved understanding the characteristics of the dataset attributes. Table 3 summarizes the features of the dataset, and Table 1 and 2 contains the descriptive statistics of the dataset.

For the comprehensive dataset analysis, the data examination predominantly relied on Python programming language and the Pandas library within the Jupyter Notebook environment.

Table 1: Descriptive Statistics of the Dataset.

	Count	Mean	Std	Min
nx	404.0000	4.0025	0.8170	3.0000
ny	404.0000	3.9975	1.4168	2.0000
nz	404.0000	4.0025	0.8170	3.0000
lx	404.0000	5.0000	0.8185	4.0000
lz	404.0000	4.9975	0.8170	4.0000
Peso	404.0000	12000.0000	0.0000	12000.0000
M_{21}	404.0000	577258.6634	209408.7459	288000.0000
M_{31}	404.0000	57725.8663	20940.8746	28800.0000
M_{22}	404.0000	576924.5049	209143.9775	288000.0000
M_{32}	404.0000	57692.4505	20914.3978	28800.0000
N_3	404.0000	2698663.3663	628660.3943	1728000.0000
N_{12}	404.0000	128279.7030	46535.2769	64000.0000
TPIANO	404.0000	1265.1609	425.0504	533.0000
M_3	404.0000	45495.6683	22821.3029	9600.0000
H_1	404.0000	0.4000	0.0000	0.4000
B_1	404.0000	0.6000	0.0000	0.6000
H_2	404.0000	0.6000	0.0000	0.6000
B_2	404.0000	0.4000	0.0000	0.6000
H_3	404.0000	0.6000	0.0000	0.6000
B_3	404.0000	0.6000	0.0000	0.6000
A_1	404.0000	0.2400	0.0000	0.2400
A_2	404.0000	0.2400	0.0000	0.2400
A_3	404.0000	0.3600	0.0000	0.3600
I_1	404.0000	0.0072	0.0000	0.0072
I_2	404.0000	0.0032	0.0000	0.0032
I_3	404.0000	0.0108	0.0000	0.0108
EM_Permanent_Load	404.0000	3.8505	0.1954	3.2168
EM_Seismic_x	404.0000	2.2121	0.4707	1.2191
EM_Seismic_y	404.0000	2.2177	0.4528	1.2285
CM_Permanent_Load	404.0000	5.9839	0.1660	5.4500
CM_Seismic_x	404.0000	2.8534	0.5882	0.0000
CM_Seismic_y	404.0000	2.7108	0.7671	0.0000

Table 2: Descriptive Statistics of the Dataset.

	25%	50%	75%	Max
nx	3.0000	4.0000	5.0000	5.0000
ny	3.0000	4.0000	5.0000	6.0000
nz	3.0000	4.0000	5.0000	5.0000
lx	4.0000	5.0000	6.0000	6.0000
lz	4.0000	5.0000	6.0000	6.0000
Peso	12000.0000	12000.0000	12000.0000	12000.0000
M_{21}	432000.0000	562500.0000	675000.0000	972000.0000
M_{31}	43200.0000	56250.0000	67500.0000	97200.0000
M_{22}	432000.0000	562500.0000	675000.0000	972000.0000
M_{32}	43200.0000	56250.0000	67500.0000	97200.0000
N_3	2160000.0000	2592000.0000	3240000.0000	3888000.0000
N_{12}	96000.0000	125000.0000	150000.0000	216000.0000
TPIANO	960.0000	1200.0000	1500.0000	2700.0000
M_3	27000.0000	43200.0000	56250.0000	145800.0000
H_1	0.4000	0.4000	0.4000	0.4000
B_1	0.6000	0.6000	0.6000	0.6000
H_2	0.6000	0.6000	0.6000	0.6000
B_2	0.4000	0.4000	0.4000	0.4000
H_3	0.6000	0.6000	0.6000	0.6000
B_3	0.6000	0.6000	0.6000	0.6000
A_1	0.2400	0.2400	0.2400	0.2400
A_2	0.2400	0.2400	0.2400	0.2400
A_3	0.3600	0.3600	0.3600	0.3600
I_1	0.0072	0.0072	0.0072	0.0072
I_2	0.0032	0.0032	0.0032	0.0032
I_3	0.0108	0.0108	0.0108	0.0108
EM_Permanent_Load	3.7808	3.9197	3.9834	4.0642
EM_Seismic_x	1.9884	2.3095	2.5811	3.0471
EM_Seismic_y	1.9089	2.2929	2.5629	3.0413
CM_Permanent_Load	5.9344	5.9736	6.1234	6.6315
CM_Seismic_x	2.5756	2.8951	3.3021	3.8555
CM_Seismic_y	2.0464	2.9081	3.3994	3.9177

3.2 Evaluation Metrics

To assess the predictive capability of the regression model for the feature $CM_Permanent_Load$, the dataset was partitioned into 70% for training and 30% for testing. The evaluation of the model's accuracy involved computing the Mean Square Error (MSE) Eq. (15), Mean Absolute Error (MAE) Eq. (16), and the Coefficient of Determination (R^2) Eq. (17).

$$MSE(y, \hat{y}) = \frac{1}{n} \sum_{i=0}^{n-1} (y_i - \hat{y}_i)^2 \quad (15)$$

Table 3: Dataset features.

Features	Unit	Description
nx	m	number of pillars in x direction, n plane
ny	m	number of pillars in y direction, n plane
nz	m	number of pillars in z direction, n plane
lx	m	span length in x direction
lz	m	span length in z direction
$Peso$	N	Self weight of the structure
$M21$	Nm	limit bending moment
$M31$	Nm	limit bending moment
$M22$	Nm	limit bending moment
$M32$	Nm	limit bending moment
$N3$	N	limit normal stress
$N12$	N	limit normal stress
$TPIANO$	N	Shear plane stress
$M3$	Nm	limit bending moment
$H1$	m	sectioned gel length
$B1$	m	sectioned gel length
$H2$	m	sectioned gel length
$B2$	m	sectioned gel length
$H3$	m	sectioned gel length
$B3$	m	sectioned gel length
$A1$	m^2	section area
$A2$	m^2	section area
$A3$	m^2	section area
$I1$	m^4	Section Inertia
$I2$	m^4	Section Inertia
$I3$	m^4	Section Inertia
$EM_Permanent_Load$	l	elastic self weight multiplier
$EM_Seismic_x$	l	elastic seismic x multiplier
$EM_Seismic_y$	l	elastic seismic z multiplier
$CM_Permanent_Load$	l	plastic self weight multiplier
$CM_Seismic_x$	l	plastic seismic x multiplier
$CM_Seismic_y$	l	plastic seismic z multiplier

$$MAE(y, \hat{y}) = \frac{1}{n} \sum_{i=0}^{n-1} |y_i - \hat{y}_i| \quad (16)$$

$$R^2(y, \hat{y}) = 1 - \frac{\sum_{i=0}^n (y_i - \hat{y}_i)^2}{\sum_{i=0}^n (y_i - \bar{y}_i)^2} \quad (17)$$

where:

- y_i denotes the predicted value;
- \hat{y}_i represents the observed value;
- $\bar{y}_i = \frac{1}{n} \sum_{k=1}^n y_i$ corresponds to the mean of the actual values.

The MAE and MSE metrics quantify the average absolute deviation and the squared deviation of predictions, respectively, while R^2 indicates the proportion of variance explained by the model, providing an overall measure of its goodness of fit.

3.3 Feature Engineering

The selection of representative features is crucial for the performance and generalization of AI models. To prevent overfitting and underfitting, a feature reduction process is applied before model implementation (Domingos, 2012; Guyon and Elisseeff, 2003). Various techniques exist for this purpose, including Principal Component Analysis (PCA), Linear Discriminant Analysis (LDA), and Pearson correlation analysis (Velliangiri et al., 2019). In this study, Pearson

correlation was employed to identify the most relevant feature set by measuring the linear association between variables. Features with a correlation coefficient above a defined threshold (e.g. $\sigma_{xy} \geq 0.85$) were removed to reduce redundancy while preserving model interpretability and robustness (Pearson, 1895).

The Pearson correlation coefficient is defined as:

$$\sigma_{xy} = \frac{cov(x,y)}{\sigma_x \sigma_y} \quad (18)$$

where $cov(x,y)$ represents the covariance between variables x and y , while σ_x and σ_y denote their respective standard deviations. Values close to +1 or -1 indicate strong positive or negative correlation, respectively, whereas values near 0 suggest no linear correlation.

3.4 Ensemble Models

For the regression task, five ensemble learning models were employed: Light Gradient-Boosting Machine (LightGBM), CatBoost, Adaptive Boosting (AdaBoost), eXtreme Gradient Boosting (XGBoost), and Random Forest (RF).

Ensemble methods, widely used in regression and classification, improve predictive accuracy by combining multiple weak learners. XGBoost enhances model performance through gradient-based optimization, while CatBoost is specifically designed for categorical data, leveraging ordered boosting to minimize target leakage (Chen and Guestrin, 2016; Prokhorenkova et al., 2018). AdaBoost prioritizes misclassified samples by iteratively adjusting instance weights (Dietterich, 2000). Random Forest, based on bootstrap aggregating, mitigates overfitting by averaging multiple decision trees (Breiman, 2001). LightGBM, similar to XGBoost, adopts a leaf-wise growth strategy to improve efficiency (Ke et al., 2017).

3.5 Post-Hoc eXplainable Artificial Intelligence Techniques Methodologies

One of the main challenges of machine learning is the lack of interpretability, which can hinder adoption, especially in critical applications. Beyond accuracy, understanding how a model makes predictions provides valuable insights. To enhance model explainability, we employed two XAI techniques: ELI5 and SHAP.

ELI5 (Explain Like I'm 5) estimates feature importance via permutation importance, measuring the impact of removing a feature on model performance.

This method, though effective, can be computationally expensive when dealing with high-dimensional datasets (eli5 Development Team, 2022).

SHAP (SHapley Additive exPlanations) offers a more granular approach by assigning importance scores to each feature for every individual prediction. This method allows for a detailed evaluation of feature contributions. In this work, we applied the TreeSHAP algorithm, optimized for decision tree-based models such as LightGBM and XGBoost (Lundberg and Lee, 2017).

4 RESULTS

4.1 Feature Engineering

Following the feature engineering process conducted using Pearson correlation, the selected features for the regression analysis are as follows: nx , ny , nz , lx , lz , $Peso$, $TPIANO$, $M3$, $H1$, $B1$, $H2$, $B2$, $H3$, $B3$, $A1$, $A2$, $A3$, $I1$, $I2$, $I3$, $EM_Permanent_load$, $EM_Seismic_y$, and $CM_Permanent_load$ has been used as target variable. These features were chosen based on their representative nature and their ability to reduce redundancy while preserving the overall explanatory power of the dataset.

4.2 Prediction

The implementation of the regression models was carried out using Python 3.9.13 and various machine learning libraries, including Sci-Kit Learn, XGBoost, CATBoost, and AdaBoost. Before presenting the regression results, it is important to note that model parameters were optimized using a k-Fold Cross Validation approach. However, for brevity, the tuned parameters are not reported in this work.

All regression models were trained with $CM_Permanent_load = y$ as the target variable, while the feature matrix X consisted of the variables described in Subsection 3.1. The evaluation metrics for each model are summarized in Table 4. The best-performing model, CATBoost, achieved $R^2 = 0.9459$, $MSE = 0.0012$, and $MAE = 0.0225$. The corresponding parity plot and error distribution are illustrated in Fig. 6.

4.3 Explainability

Table 5 reports the results of permutation importance computed through the ELI5 algorithm. The features that have the highest impact on the prediction of

Table 4: Evaluation Metrics.

Model	R^2	MSE	MAE
CATBoost	0.9459	0.0012	0.0225
XGBoost	0.9391	0.0014	0.0157
RF	0.9294	0.0016	0.0201
LightGBM	0.8538	0.0033	0.0405
ADABOOST	0.7327	0.0061	0.0590

Table 5: Permutation Importance (Weight) and Standard Deviation (St.Dev.) for All Features (ELI5 Algorithm). Features are ranked by importance.

Feature	Weight	St.Dev.
ny	0.6492	0.0500
nz	0.6235	0.1037
nx	0.5670	0.1168
lx	0.2168	0.0255
$EM_Permanent_load$	0.1874	0.0246
$EM_Seismic_y$	0.0322	0.0061
$M3$	0.0177	0.0112
$TPIANO$	0.0075	0.0026
$H1$	0.0000	0.0000
$B1$	0.0000	0.0000
$H2$	0.0000	0.0000
$Peso$	0.0000	0.0000
$H3$	0.0000	0.0000
$B3$	0.0000	0.0000
$A1$	0.0000	0.0000
$A2$	0.0000	0.0000
$A3$	0.0000	0.0000
$I1$	0.0000	0.0000
$I2$	0.0000	0.0000
$I3$	0.0000	0.0000
$B2$	0.0000	0.0000
lz	-0.0048	0.0025

$CM_Permanent_load$ values are related to the structural parameters, particularly ny , nz , and nx , which rank as the top three in terms of permutation importance. Conversely, lx and $EM_Permanent_load$ show moderate contributions, while lz has a negligible effect, as indicated by its low importance score.

However, permutation importance only highlights the degree to which features affect the predictions, without illustrating how the predicted value changes as feature values vary. To address this limitation, SHAP values were calculated, and the corresponding SHAP summary plot is shown in Figure 7.

The SHAP summary plot provides insight into both the magnitude and direction of feature contributions to the predictions.

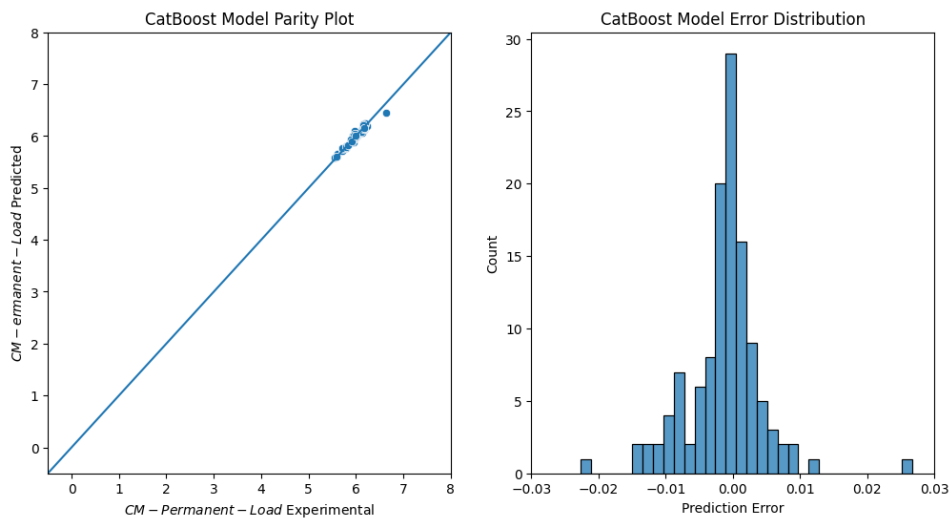


Figure 6: CATBoost Model Parity Plot and Error Distribution.

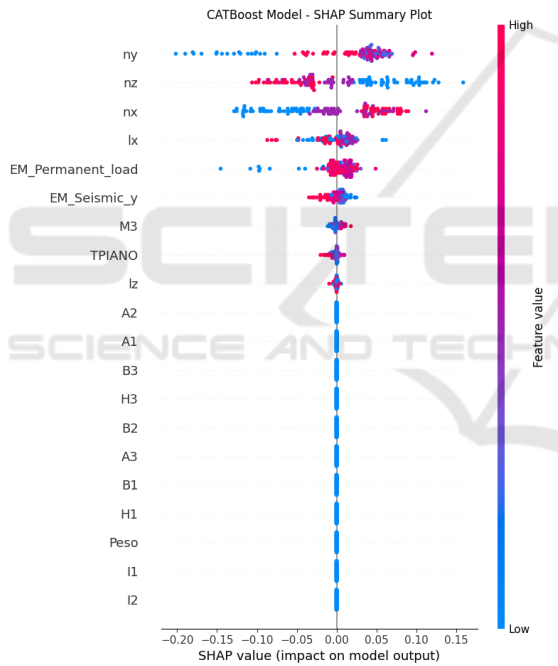


Figure 7: SHAP Values Summary Plot for CATBoost Model.

5 DISCUSSION

Understanding the vulnerability of this system makes it possible to plan targeted interventions, with the aim of reducing or managing specific criticalities through a prioritised programme of action, thus improving the resilience and overall efficiency of the built fabric against natural disasters. This system allows a vulnerability class to be assigned to each building through

a simplified analysis and quick consultation of predefined schemes. The adoption of this classification allows a quantitative assessment of structural performance and is becoming a reference for future regulations. The proposed work aims to define a protocol for disaster mitigation and prevention through a numerical approach based on an analytical analysis of structural capacity curves. The main innovation of the approach lies in the analysis method adopted, which is based on a discontinuous finite element algorithm that has already been extensively validated on various case studies. This method provides direct and generalisable results based on the structural morphology of buildings. The canonical methods, which are based on a direct mechanical analysis of the seismic capacity of individual or aggregated buildings, while reliable, require a high level of knowledge of the structures and a high computational cost, making them impractical for urban-scale assessments. However, recent developments in seismic risk and vulnerability classification methodologies have made it possible to adopt a more rapid approach that allows direct estimation of building damage following seismic events and identification of the most appropriate mitigation measures. In this project, mechanical analysis models are integrated with data obtained from monitoring, allowing quantitative and qualitative information useful for risk management to be obtained. The approach proposed for the Mitigation and Prevention Protocol overcomes the problem of the high computational cost of the techniques currently used. The work proposes to define the non-linear behaviour of a random sample of buildings through a simplified pushover procedure based on limit analysis. The integration of machine learning techniques in the structural vulner-

ability assessment process and in the definition of the Mitigation and Prevention Protocol introduces significant advantages in terms of efficiency, scalability and accuracy of the analysis. The use of advanced machine learning algorithms makes it possible to process large volumes of data from structural monitoring, geospatial surveys and seismic event histories, allowing correlations to be identified that are not immediately detectable with traditional methods. One of the main benefits of using machine learning is the ability to automate the classification of the seismic vulnerability of buildings based on geometric, material and construction characteristics, reducing the margin of error associated with subjective assessments and approximations of deterministic models. Deep learning algorithms, trained on extensive datasets, can improve the prediction of damage scenarios through the analysis of satellite images, LIDAR data and information from sensors distributed in buildings. This approach enables rapid assessments on a large scale, facilitating the planning of targeted preventive interventions and optimising the allocation of resources. Furthermore, the implementation of predictive models based on neural networks and advanced regression techniques allows the estimation of structural capacity curves to be refined, improving the accuracy of simplified pushover analysis. Through supervised learning, it is possible to develop early warning systems capable of recognising premonitory signals of structural failure in real time, increasing the safety level of buildings and urban infrastructure.

6 CONCLUSIONS

The use of machine learning (ML) models in the assessment of the seismic vulnerability of buildings is motivated by the need to develop efficient predictive tools, capable of processing large volumes of data and adapting to variable conditions without the need for simplifying assumptions imposed by traditional methods. Compared to purely physical approaches, such as finite element simulations, ML models allow for a significant reduction in calculation time, making it possible to analyse a large number of structures in a short period of time. Furthermore, the ability of ML models to learn directly from experimental and numerical data allows for the identification of complex patterns that might not be immediately evident in models based exclusively on mechanical principles. Compared to traditional statistical methods, machine learning offers greater flexibility and generalisation capacity, reducing dependence on linear or parametric assumptions. Integration with a physics-

based approach, based on the lower limit theorem of limit analysis, also guarantees respect for the fundamental principles of structural mechanics, mitigating the risk of obtaining predictions without a physical basis. This combination of advantages makes the proposed approach particularly suitable for tackling the problem of assessing seismic vulnerability in a more efficient, robust and scalable way compared to alternative approaches. Finally, the combined use of machine learning with traditional numerical methodologies helps to reduce the processing time and computational cost of analyses, making assessments more accessible even for large and complex urban contexts. This synergy between artificial intelligence and structural engineering represents a decisive step towards the creation of more resilient built environments capable of dynamically adapting to the stresses induced by extreme events.

REFERENCES

- Alber, M., Tepole, A. B., Cannon, W. R., De, S., Dura-Bernal, S., Garikipati, K., Karniadakis, G., Lytton, W. W., Perdikaris, P., Petzold, L., and Kuhl, E. (2019). Integrating machine learning and multiscale modeling—perspectives, challenges, and opportunities in the biological, biomedical, and behavioral sciences.
- Barredo Arrieta, A., Díaz-Rodríguez, N., Del Ser, J., Benetot, A., Tabik, S., Barbado, A., Garcia, S., Gil-Lopez, S., Molina, D., Benjamins, R., Chatila, R., and Herrera, F. (2020). Explainable artificial intelligence (xai): Concepts, taxonomies, opportunities and challenges toward responsible ai. *Information Fusion*, 58:82–115.
- Breiman, L. (2001). Random forests. *Machine Learning*, 45(1):5 – 32.
- Campanile, L., Di Bonito, L. P., Iacono, M., and Di Natale, F. (2023). Prediction of chemical plants operating performances: a machine learning approach. In *Proceedings - European Council for Modelling and Simulation, ECMS*, volume 2023-June, page 575 – 581.
- Campanile, L., Di Bonito, L. P., Natale, F. D., and Iacono, M. (2024). Ensemble models for predicting co concentrations: Application and explainability in environmental monitoring in campania, italy. In *Proceedings - European Council for Modelling and Simulation, ECMS*, volume 38, page 558 – 564.
- Chen, T. and Guestrin, C. (2016). Xgboost: A scalable tree boosting system. In *Proceedings of the ACM SIGKDD International Conference on Knowledge Discovery and Data Mining*, volume 13-17-August-2016, page 785 – 794.
- Ciaccio, F. D. and Troisi, S. (2021). Monitoring marine environments with autonomous underwater vehicles: A bibliometric analysis.
- Damiano, E., Battipaglia, M., de Cristofaro, M., Ferlisi, S., Guida, D., Moliterno, E., Netti, N., Valiante, M., and

- Olivares, L. (2024). Innovative extenso-inclinometer for slow-moving deep-seated landslide monitoring in an early warning perspective. *JOURNAL OF ROCK MECHANICS AND GEOTECHNICAL ENGINEERING*.
- de Cristofaro, M., Asadi, M. S., Chiaradonna, A., Damiano, E., Netti, N., Olivares, L., and Orense, R. (2024). Modeling the excess porewater pressure buildup in pyroclastic soils subjected to cyclic loading. *JOURNAL OF GEOTECHNICAL AND GEOENVIRONMENTAL ENGINEERING*, 150.
- Di Bonito, L. P., Campanile, L., Di Natale, F., Mastroianni, M., and Iacono, M. (2024). explainable artificial intelligence in process engineering: Promises, facts, and current limitations. *Applied System Innovation*, 7(6).
- Di Bonito, L. P., Campanile, L., Napolitano, E., Iacono, M., Portolano, A., and Di Natale, F. (2023). Analysis of a marine scrubber operation with a combined analytical/ai-based method. *Chemical Engineering Research and Design*, 195:613 – 623.
- Dietterich, T. G. (2000). Ensemble methods in machine learning. *Lecture Notes in Computer Science (including subseries Lecture Notes in Artificial Intelligence and Lecture Notes in Bioinformatics)*, 1857 LNCS:1 – 15.
- Domingos, P. (2012). A few useful things to know about machine learning. *Commun. ACM*, 55(10):78–87.
- eli5 Development Team (Accessed 2022). *eli5 Documentation - Permutation Importance*.
- Gunning, D. and Aha, D. W. (2019). Darpa's explainable artificial intelligence program. *AI Magazine*, 40(2):44–58.
- Guyon, I. and Elisseeff, A. (2003). An introduction to variable and feature selection. *J. Mach. Learn. Res.*, 3(null):1157–1182.
- Karpatne, A., Atluri, G., Faghmous, J. H., Steinbach, M., Banerjee, A., Ganguly, A., Shekhar, S., Samatova, N., and Kumar, V. (2017). Theory-guided data science: A new paradigm for scientific discovery from data. *IEEE Transactions on Knowledge and Data Engineering*, 29.
- Ke, G., Meng, Q., Finley, T., Wang, T., Chen, W., Ma, W., Ye, Q., and Liu, T.-Y. (2017). Lightgbm: A highly efficient gradient boosting decision tree. In *Advances in Neural Information Processing Systems*, volume 2017-December, page 3147 – 3155.
- Laub, J. A. (1999). Assessing the servant organization; development of the organizational leadership assessment (ola) model. dissertation abstracts international., *Procedia - Social and Behavioral Sciences*, 1.
- Lundberg, S. M. and Lee, S.-I. (2017). A unified approach to interpreting model predictions. In *Advances in Neural Information Processing Systems*, volume 2017-December, page 4766 – 4775.
- Malami, S. I., Anwar, F. H., Abdulrahman, S., Haruna, S. I., Ali, S. I. A., and Abba, S. I. (2021). Implementation of hybrid neuro-fuzzy and self-turning predictive model for the prediction of concrete carbonation depth: A soft computing technique. *Results in Engineering*, 10.
- Mangalathu, S., Hwang, S.-H., and Jeon, J.-S. (2020). Machine learning-based failure mode identification of reinforced concrete shear walls. *Engineering Structures*, 207:110257.
- McGovern, A., Lagerquist, R., Gagne, D. J., Jergensen, G. E., Elmore, K. L., Homeyer, C. R., and Smith, T. (2019). Making the black box more transparent: Understanding the physical implications of machine learning. *Bulletin of the American Meteorological Society*, 100.
- Momeny, M., Latif, A. M., Sarram, M. A., Sheikhpour, R., and Zhang, Y. D. (2021). A noise robust convolutional neural network for image classification. *Results in Engineering*, 10.
- Pearson, K. (1895). Note on regression and inheritance in the case of two parents. *Proc. R. Soc. Lond.*, 58:240–242.
- Prokhorenkova, L., Gusev, G., Vorobev, A., Dorogush, A. V., and Gulin, A. (2018). Catboost: Unbiased boosting with categorical features. In *Advances in Neural Information Processing Systems*, volume 2018-December, page 6638 – 6648.
- Santhosh, A. J., Tura, A. D., Jiregna, I. T., Gemechu, W. F., Ashok, N., and Ponnusamy, M. (2021). Optimization of cnc turning parameters using face centred ccd approach in rsm and ann-genetic algorithm for aisi 4340 alloy steel. *Results in Engineering*, 11.
- Sharma, D. K., Jalil, N. A., Nassa, V. K., Vadyala, S. R., Senthamil, L. S., and Thangadurai, N. (2021). Deep learning applications to classify cross-topic natural language texts based on their argumentative form. In *Proceedings - 2nd International Conference on Smart Electronics and Communication, ICOSEC 2021*.
- Vadyala, S. R., Betgeri, S. N., and Betgeri, N. P. (2022). Physics-informed neural network method for solving one-dimensional advection equation using pytorch. *Array*, 13.
- Vadyala, S. R., Betgeri, S. N., Sherer, E. A., and Amritphale, A. (2021). Prediction of the number of covid-19 confirmed cases based on k-means-lstm. *Array*, 11.
- Vadyala, S. R. and Sherer, E. A. (2021). Natural language processing accurately categorizes indications, findings and pathology reports from multicenter colonoscopy: Qualitative focus study (preprint). *JMIR Cancer*.
- Velliangiri, S., Alagumuthukrishnan, S., and Thankumar joseph, S. I. (2019). A review of dimensionality reduction techniques for efficient computation. *Procedia Computer Science*, 165:104–111.
- Zona, R., Ferla, P., and Minutolo, V. (2021). Limit analysis of conical and parabolic domes based on semi-analytical solution. *Journal of Building Engineering*, 44.
- Zona, R. and Minutolo, V. (2024). A dislocation-based finite element method for plastic collapse assessment in solid mechanics. *Archive of Applied Mechanics*.